

# Correlations of conductance peaks and transmission phases in deformed quantum dots

Reinhard Baltin<sup>1</sup>, Yuval Gefen<sup>2</sup>, Gregor Hackenbroich<sup>1,3</sup>, and Hans A. Weidenmüller<sup>1</sup>

<sup>1</sup>*Max Planck Institut für Kernphysik, Postfach 103980, 69029 Heidelberg, Germany*

<sup>2</sup>*Department of Condensed Matter Physics,*

*The Weizmann Institute of Science, 76100 Rehovot, Israel*

<sup>3</sup>*Universität GH Essen, Fachbereich 7, 45117 Essen, Germany*

(February 17, 2018)

## Abstract

We investigate the Coulomb blockade resonances and the phase of the transmission amplitude of a deformed ballistic quantum dot weakly coupled to leads. We show that preferred single-particle levels exist which stay close to the Fermi energy for a wide range of values of the gate voltage. These states give rise to sequences of Coulomb blockade resonances with correlated peak heights and transmission phases. The correlation of the peak heights becomes stronger with increasing temperature. The phase of the transmission amplitude shows lapses by  $\pi$  between the resonances. Implications for recent experiments on ballistic quantum dots are discussed.

PACS numbers: 73.23.Hk, 73.23.Ps, 73.40.Gk

## I. INTRODUCTION

Quantum dots have been intensively investigated both experimentally and theoretically [1] in recent years. In this paper, we present a theoretical study of the correlations of conductance peaks and of transmission phases that have been observed in recent experiments on quantum dots in the Coulomb blockade regime.

Quantum dots are small islands of electrons that are only a few hundred nanometers in size and typically contain a few hundred electrons. The spectrum of a quantum dot is determined by the Coulomb interaction of the electrons and by the external electrostatic confining potential. The confining potential and hence the size and shape of a quantum dot can be controlled by external gates. This makes quantum dots an ideal tool for studying the properties of finite systems of interacting fermions.

Experimentally, the spectra of quantum dots have been measured using optical (far-infrared) spectroscopy and/or transport experiments. In the latter case, the quantum dot is coupled via tunnel barriers to external leads. The conductance measured at a finite drain-source voltage reveals the excitation spectrum of the dot whereas the linear conductance yields the addition spectrum of the quantum dot. Both the excitation and the addition spectrum are dominated by the classical Coulomb blockade effect: Large conductance peaks are observed when the dot potential is tuned in such a way that the number of electrons on the dot can fluctuate without any cost in energy. These peaks are nearly periodic in the gate voltage on the dot. At consecutive peaks the number of electrons on the dot changes by one. At values of the gate voltage located between the positions of the conductance peaks, electron transport through the dot requires a large charging energy. Hence, the current between conductance peaks is strongly suppressed, the remaining current being mostly due to virtual tunneling processes (co-tunneling regime) [2].

Typically, metallic quantum dots have such a large density of states that the Coulomb blockade oscillations can be described by classical theory which ignores the discreteness of the spectrum. The situation is different in semiconductor dots. Here, the mean single-

particle level spacing  $\Delta$  can be larger than the temperature  $kT$ . The regime  $\Delta \gg kT, \Gamma$ , where  $\Gamma$  is the strength of the coupling to the leads, is the resonant tunneling regime. In this regime, each conductance peak is mediated by a single quantum state of the dot. The peak height of the conductance resonance is a direct signature of the wave function of the resonant state.

Some years ago, Jalabert, Stone, and Alhassid developed a statistical theory of the Coulomb blockade [3] in the resonant tunneling regime. In order to explain strong fluctuations of the peak heights of neighboring conductance resonances, they assumed that the eigenstates of a quantum dot can be described by random matrix theory. According to this theory no correlations are to be expected for the peak heights of neighboring peaks. Moreover, the distribution of peak heights is predicted to be universal, and only determined by the fundamental symmetries of the system. While two recent experiments [4,5] appeared to have confirmed these predictions, a more careful examination of the experimental data casts some doubt on the validity of random matrix theory in describing the physics of quantum dots. Deviations from the predictions of random matrix theory include the appearance of 4-5 correlated transmission peaks [5], non Wigner-Dyson related distribution of conductance peak spacing [6,7], and reduced sensitivity to magnetic flux [4,5,7,8]. Even stronger correlations have been reported in very recent experiments using a quantum dot embedded in an Aharonov-Bohm ring [9] where both the peak heights and the phase of the transmission amplitude could be measured. Strong correlations within sequences of more than 10 resonances were found.

In the experiments of Refs. [4,5,7,9],  $kT$  was approximately  $(0.1 - 0.5)\Delta$ . When the resonant tunneling limit  $\Delta \gg kT$  is not fully met, also neighboring eigenstates around the Fermi energy (rather than only a single state) contribute to the conductance peak. Extending the random matrix theory description to the regime  $\Delta > kT$ , correlations in the peak height were found [10]. Those temperature-induced correlations seem sufficiently strong to account for sequences of up to 5 correlated peaks as reported in Ref. [5]. However, temperature alone can clearly be ruled out as the source of the much stronger correlations found in Ref. [9]. A

mechanism different from and acting in addition to temperature must be the origin of these correlations.

In this paper we propose such a mechanism. Our model involves certain geometry-specific assumptions and is therefore restricted in generality and universality. Nevertheless it may still pertain to experiments on nearly integrable ballistic dots (cf. Section III). Our mechanism is a synthesis of two approaches developed earlier [11,12]. In Ref. [11] a scenario was described for peak correlations at *vanishing temperature*. It was argued that deformation of the confining potential of the dot generically gives rise to avoided crossings of the single-particle levels on the dot. As a result of such crossings one and the same eigenstate of the dot may dominate a sequence of neighboring conductance peaks [11] and thereby cause correlations. Although several arguments in support of this mechanism were given [11], a quantitative study of the resulting correlations has not been presented yet. A different line of thought was pursued in Ref. [12]. That paper aimed at explaining the "phase lapse" observed in the experiment of Ref. [9] (a different theoretical discussion of the phase lapse was presented in Ref. [13]). It was shown [12] that the phase-lapse behavior as well as strong *finite temperature* correlations of conductance peaks arise if the dot supports one particularly well conducting state. This state would dominate a sequence of conductance peaks provided it remained within an energy interval of order  $kT$  around the Fermi energy.

Here we study peak-height correlations and the transmission phase in quantum dots taking a deformed harmonic oscillator as a specific example. Using this model, we show that deformation of the confining potential leads to peak-height correlations, in keeping with the arguments of Ref. [11]. We identify those eigenstates of the quantum dot that are most strongly coupled to the external leads and which, therefore, support the bulk of the current through the dot. Peak-height correlations are strongest for sequences of resonances mediated by such states. We also investigate the influence of temperature on the correlations. As expected from the studies in Ref. [12], we find that temperature leads to a marked increase of the correlations. Combining the effect of deformation and of temperature, we obtain sequences of up to 30 conductance resonances with similar transmission phases

and similar peak heights. We demonstrate that this same mechanism may also account for the phase-lapse behavior observed in Ref. [9].

The paper is organized as follows: In the next Section we introduce a model for a deformed quantum dot and describe how correlations can arise. In Section 3 we calculate the conductance with the help of a master equation. In Section 4 we investigate the transmission phase. This phase can be measured in Aharonov–Bohm type experiments containing a quantum dot. The last Section gives a summary and a discussion of the limitations of our model.

## II. THE MODEL

The confining potential of a quantum dot is often defined electrostatically in terms of a split gate. As depicted in Figure 1, this is an arrangement of electrodes on the surface of a heterostructure. When a negative bias is applied to the gates, the two-dimensional electron gas located some 100 nm or so beneath the electrodes will be depleted. The barriers through which electrons can tunnel between the leads and the dot are denoted by  $A$  and  $B$ . A voltage  $V_g$  applied to the plunger gate  $P$  controls the chemical potential on the dot. A change of  $V_g$  not only changes the number of electrons on the dot but also distorts the confining potential of the two-dimensional electron gas in a substantial way, causing a deformation of the quantum dot [11].

We consider the standard Hamiltonian  $H$  for a quantum dot coupled to leads, containing the Hamiltonians  $H^L$  and  $H^R$  of the left and right leads, respectively, the Hamiltonian of the isolated quantum dot  $H^D$ , and the Hamiltonian  $H^T$  for tunneling between the leads and the dot,

$$H = H^L + H^R + H^D + H^T ,$$

$$H^{L(R)} = \sum_k \epsilon_k^{L(R)} a_k^{L(R)\dagger} a_k^{L(R)} ,$$

$$H^D = \sum_n \epsilon_n c_n^\dagger c_n + \frac{1}{2} U \hat{N}(\hat{N} - 1) ,$$
(1)

$$H^T = \sum_{n,k} \left( V_{n,k}^L a_k^L c_n^\dagger + \text{h.c.} \right) + \sum_{n,k} \left( V_{n,k}^R a_k^R c_n^\dagger + \text{h.c.} \right) .$$

Here,  $\epsilon_k^{L,R}$  and  $\epsilon_n$  are the energies and  $a_k^{L,R}$  and  $c_n$  the annihilation operators for single-particle states in the leads and in the dot, respectively. For the Coulomb interaction on the quantum dot we use the constant interaction model with  $\hat{N} = \sum_n n_n$  the number of electrons on the quantum dot. The tunneling matrix elements  $V_{i,k}^{L(R)}$  involve the overlap of wave functions in the leads and in the dot and are given below.

We model the confining potential as an anisotropic harmonic oscillator potential. A harmonic potential has been used previously in studies of quantum dots [14] and, at least for small dots, is believed to be a fair approximation to the true confining potential. Although we use a specific model, most of our conclusions apply to any sufficiently smooth confining potential for which the Hamiltonian is nearly integrable. Then, the transverse and longitudinal modes in the dot are nearly decoupled, cf. Eq. (2). This condition is met when the matrix elements of the perturbation violating integrability are smaller than the mean single-particle level spacing. However, even mild disorder or boundary roughness violating this condition will modify our picture considerably.

The energy eigenvalues  $\epsilon_n$  for the quantum numbers  $n = (n_x, n_y)$  are given by

$$\epsilon_n = E(n_x, n_y) = \hbar\omega_x(n_x + \frac{1}{2}) + \hbar\omega_y(V_g)(n_y + \frac{1}{2}) - \alpha V_g + E_0. \quad (2)$$

To describe the deformation, we assume that the oscillator frequency  $\omega_y(V_g) = \omega_x(1 - \gamma(V_g - V_0))$  in the transverse direction  $y$  depends linearly on the gate voltage  $V_g$  while the frequency  $\omega_x$  in the longitudinal  $x$ -direction is held fixed. The parameter  $\alpha$  relates the overall depth of the dot's potential to the gate voltage. The constants  $E_0$  and  $V_0$  determine the number of electrons on the dot at zero deformation.

The dependence of the single-particle levels on the gate voltage is shown in Figure 2. The shell structure of the isotropic harmonic oscillator ( $V_g = V_0$ ) is clearly visible. It survives for small values of  $V_g$  but is eventually destroyed by deformation. Each shell  $q$  is characterized by non-negative integer quantum numbers  $q = n_x + n_y$ . In each shell, there

are levels depending weakly (strongly) on  $V_g$ , characterized by large (small) values of  $n_x$  and small (large) values of  $n_y$ , respectively. These are referred to as “flat levels” and “steep levels”, respectively. A small deviation from integrability will change the level crossings shown in Figure 2 into avoided crossings. For nearly integrable systems, the wave functions retain their character across avoided crossings. Flat levels are particularly stable, their wave functions change little with deformation (or gate voltage) and remain self-similar even after several avoided crossings [11].

The matrix elements  $V^L, V^R$  for tunneling from the left and right lead to the quantum dot are given by [15]

$$V^{L(R)}(k, n_x, n_y) = \frac{\hbar^2}{2m} \int_B dy \left[ \psi_k(x, y)^* \frac{\partial \Phi_{n_x, n_y}(x, y)}{\partial x} - \Phi_{n_x, n_y} \frac{\partial \psi_k(x, y)^*}{\partial x} \right]_{x=x_B}. \quad (3)$$

Here  $\psi_k^{L(R)}$  is the wave function with wave vector  $k$  in the left (right) lead, and  $\Phi_{n_x, n_y}$  is the wave function in the dot. The integration extends in the  $y$ -direction and  $x_B$  is arbitrary but must be located within the barrier [15]. We restrict ourselves to the case of a single transverse channel in each lead. The nodes of the wave functions of flat (steep) levels with large  $n_x$  ( $n_y$ ) are predominantly carried by the x-component (y-component, respectively). Thus, the wave functions of flat levels extend much further into the barrier region and have considerably larger matrix elements  $V^{L(R)}(k, n_x, n_y)$  than those of the steep levels. This important property is illustrated in Figure 3. It has immediate consequences for the conductance at finite temperature: The very same single-particle state can dominate different Coulomb blockade resonances seen at different values of  $V_g$  [11]. We now explain this feature qualitatively, postponing a detailed discussion to later sections.

At low temperature ( $kT \ll \Delta$ ) and for small bias voltage, the transmission through the dot can be qualitatively obtained from the mean-field approximation for the dot spectrum. In this approximation, each single-particle energy  $\epsilon_i$  is replaced by the effective value  $\varepsilon_i = \epsilon_i + U \sum_{j \neq i} \langle n_j \rangle$  [16,17]. According to Koopmans’ theorem,  $\varepsilon_i$  is the energy needed to add an electron in state  $i$  to the dot, whereas the excitation energy at fixed electron number is given by the difference of the corresponding two effective energies. Because of the Coulomb

interaction, there is a gap of magnitude  $U$  between the last occupied and the first empty effective single-particle level, while the other occupied (empty) levels below (above) the Fermi energy  $E_F$  are on average separated by the usual mean level spacing  $\Delta$ . Avoided crossings of single-particle levels result in avoided crossings of the effective levels, in spite of this gap [11].

A Coulomb blockade resonance occurs, and the number of electrons on the dot changes by one, whenever an effective single-particle level crosses the Fermi energy  $E_F$  of the reservoirs. (We assume  $E_F$  to be independent of the gate voltage in the following). For  $U \gg \Delta$ , the distance between adjacent resonances is  $\delta V_g = U/\alpha$ . Without level crossings, different resonances correspond to different single-particle levels. In the presence of level crossings, the situation changes. This is shown in Figure 4 which displays the gap between the filled levels below and the empty ones above  $E_F$ . Resonances occur at gate voltages  $V_1, V_2$  and  $V_3$ . Suppose a flat level  $F$  (dashed) crosses  $E_F$  at  $V_1$ . If there is an avoided crossing of  $F$  with a steep level  $S_1$  from a higher shell between  $V_1$  and  $V_2$ , level  $F$  is pushed above  $E_F$  while level  $S_1$  is immersed into the Fermi sea. At  $V_2$  the flat level  $F$  crosses  $E_F$  again, causing another resonance to occur. The mechanism works again between  $V_2$  and  $V_3$  where another steep level  $S_2$  intersects with  $F$ . Since flat levels keep their wave functions after avoided crossings, the resonances at  $V_1, V_2$  and  $V_3$  all carry the *same* single-particle wave function. This mechanism gives rise to strong correlations of the properties (peak height and transmission phase) of several resonances. However, it leads to strong correlations only if there is *one and only one* crossing of the flat level  $F$  with a steep level within subsequent intervals  $\delta V_g$ . If – on average – there is less than one (more than one) crossing, the level  $F$  will eventually be pulled down below (up above) the Fermi energy and will become irrelevant for the behavior of Coulomb blockade resonances.

So far, we have focussed attention on the resonant tunneling regime  $\Gamma, kT \ll \Delta$  where only the level *at* the Fermi energy determines the properties of the resonance. Essential modifications arise for finite temperatures  $kT \sim \Delta$ . Here, also levels at a distance  $\sim kT$  from  $E_F$  contribute to the resonance. Since the flat levels are coupled to the leads much

more strongly than the steep ones, the presence of a flat level at a distance  $\sim kT$  from  $E_F$  suffices for it to dominate the resonance. Long sequences of correlated resonances may occur if repeated avoided crossings cause a flat level  $F$  to stay sufficiently close to  $E_F$  over a sufficiently long range of  $V_g$  values. This is the picture we investigate quantitatively for the case of an anharmonic oscillator in the sequel. The picture suggests that the correlations of consecutive Coulomb blockade resonances will increase with temperature.

The number of intersection points of a flat level ( $n_x \neq 0, n_y = 0$ ) with steep levels from higher shells can be determined from Eq. (2). The total number of crossings of the flat level occurring in the range  $V_g - V_0$  is given by

$$N_c = \frac{n_x^2}{2} \frac{\gamma(V_g - V_0)}{1 - \gamma(V_g - V_0)}. \quad (4)$$

The number of steep levels from higher shells increases with deformation and causes  $N_c$  to increase, too, until it diverges for the unphysical situation of extreme deformation  $\omega_y \rightarrow 0$ . In order to have one crossing within an interval  $\delta V_g = U/\alpha$  we require  $(\partial N_c)/(\partial V_g) = \alpha/U$ . This condition yields the value of  $V_g$  where maximal correlations between Coulomb blockade resonances should occur. We estimate the number  $\Delta N$  of resonances for which the distance between the flat level ( $n_x, 0$ ) and the Fermi energy is less than one level spacing and obtain

$$\Delta N \simeq 2 \sqrt{n_x \sqrt{\frac{\alpha}{2\gamma U}}}, \quad (5)$$

with a deformation  $\omega_y/\omega_x = \sqrt{(\gamma U)/(2\alpha)} n_x$ .

### III. COULOMB BLOCKADE RESONANCES

In this section we calculate the conductance  $G$  of a quantum dot with the single-particle spectrum (2) in linear response. We use the master equation [18]. In the Coulomb blockade regime, maxima in  $G$  occur for values of  $V_g$  where the configurations with  $N$  and  $N + 1$  electrons on the dot are degenerate. The resulting sharp conductance peaks are almost equally spaced [1,18]. For  $kT \ll \Delta$  each peak is due to a single level  $n$  of the dot, and

the peak height is given by  $G \sim \Gamma_n^L \Gamma_n^R / (\Gamma_n^L + \Gamma_n^R)$  [18] with the tunneling rates  $\Gamma_n^{L(R)} \sim \sum_k |V_{k,n}^{L(R)}|^2 \delta(\epsilon_n - \epsilon_k^{L(R)})$ . We note that the peak heights are highly sensitive to the wave functions in the dot. Strongly coupled levels give higher peaks than the weakly coupled ones. For finite temperature several single-particle states contribute to a resonance.

Under the assumption of sequential tunneling, transport through the dot at finite temperature is described by the master equation [18]. In the regime  $kT \gg \Gamma$  this equation determines the occupation probabilities  $P_\nu$  of the single-particle levels of the dot under the influence of the interaction  $U$  and of the coupling to the leads. It is given by

$$\frac{\partial}{\partial t} P_\nu = \sum_{\mu(\neq\nu)} P_\mu \Gamma_{in}(\mu \rightarrow \nu) - P_\nu \Gamma_{out}(\nu \rightarrow \mu) . \quad (6)$$

Here  $\mu$  and  $\nu$  label Fock states, i.e., Slater determinants defined in terms of the occupation numbers of all single-particle states in the dot. The symbols  $\Gamma_{in}$  and  $\Gamma_{out}$  stand for the rates of the tunneling processes into and out of the dot. These processes change the number of electrons on the dot by one, and the associated Fock states from  $\mu$  to  $\nu$ , and vice versa. The rates contain not only the coupling of the specific single-particle states of the dot to the leads but also take into account a possible suppression of tunneling by the occupation of the states in the leads. By expanding Eq. (6) around the equilibrium probability distribution Beenakker [18] obtained the conductance  $G$  for small bias voltage,

$$G = \frac{e^2}{kT} \sum_n \sum_{N=1}^{\infty} \frac{\Gamma_n^L \Gamma_n^R}{\Gamma_n^L + \Gamma_n^R} P_N^{\text{eq}} [1 - F^{\text{eq}}(\epsilon_n | N)] f(\epsilon_n + U \cdot N) . \quad (7)$$

Here,  $f$  is the Fermi function and  $P_N^{\text{eq}}$  is the probability to find  $N$  electrons on the dot,

$$P_N^{\text{eq}} = \frac{\text{tr}_N \exp(-\beta H^D)}{\text{tr} \exp(-\beta H^D)} = \frac{\text{tr}_N \exp(-\beta H^D)}{\sum_N \text{tr}_N \exp(-\beta H^D)} . \quad (8)$$

The inverse temperature is denoted by  $\beta$ , and  $\text{tr}_N$  denotes the trace over the Fock states with  $N$  electrons on the dot. The canonical occupation number of level  $n$  when there are  $N$  electrons on the dot is given by

$$F^{\text{eq}}(\epsilon_n | N) \equiv \langle \hat{n}_n \rangle_N = \frac{\text{tr}_N (n_n \exp(-\beta H^D))}{\text{tr}_N \exp(-\beta H^D)} . \quad (9)$$

Eqn. (7) has also been derived [19] using a Landauer–Büttiker type approach generalized to include the interaction of electrons on the dot.

Numerically, it turns out to be sufficient to calculate  $F^{\text{eq}}(\epsilon_n|N)$  for a window of levels around the Fermi energy, and to take the occupation numbers equal to 1 below and 0 above this window. The following results are obtained using a window of 16 levels that are populated with 8 electrons. We checked that our results are insensitive to changes of the window size.

Using Eq. (3) and the relation  $\Gamma_n^{L(R)} \sim \sum_k |V_{k,n}^{L(R)}|^2 \delta(\epsilon_n - \epsilon_k^{L(R)})$ , we find that the tunneling rates  $\Gamma_n$  are proportional to the square modulus of the harmonic oscillator wave functions at the position of the barriers  $\vec{r} = (x_B, y_B)$ ,

$$\Gamma_n \sim \frac{(H_{n_x}(\xi_x) H_{n_y}(\xi_y))^2}{2^{(n_x+n_y)} n_x! n_y!} e^{-(\xi_x^2 + \xi_y^2)}, \quad (10)$$

where  $H_n$  are the Hermite polynomials and where we have used dimensionless variables  $\xi_x = \sqrt{m\omega_x/\hbar} x_B$  and  $\xi_y = \sqrt{m\omega_y/\hbar} y_B$ . Neglecting deformation we can relate the barrier height  $V_B$  to the position of the barrier via  $V_B/\hbar\omega_x = (\xi_x^2 + \xi_y^2)/2$ . In the sequel we choose a fixed value  $V_B/\hbar\omega = 25$  for the barrier height.<sup>1</sup> We consider two different geometries of the leads connecting the quantum dot with external reservoirs: (i) The two leads are located exactly opposite to each other, so that  $\xi_x = \pm\sqrt{50}$  and  $\xi_y = 0$ . (ii) The leads are arranged at an angle of 90 degrees, with the barriers at  $\xi_x = \xi_y = -\sqrt{50/2}$  and  $\xi_x = -\xi_y = \sqrt{50/2}$ . The latter geometry has been used, for instance, in the experiment of Ref. [5].

The tunneling rates  $\Gamma_n$  for both geometries and for several states  $n$  are presented in

---

<sup>1</sup>Compared with typical experimental parameters this value appears to be too small. We use this value in order to avoid an unphysically large increase of  $\Gamma$  with increasing quantum number  $n_x$ . Such a strong increase is characteristic of the harmonically shaped barrier. A less steep increase would be obtained for steeper tunneling barriers. Such barriers appear to give a more realistic description of the depletion zone of the electron gas near the gates. For reasons of consistency with the harmonic oscillator model used throughout this paper, we decided to use harmonic barriers.

Table I. We note that for geometry (i) the flat levels are coupled much more strongly to the leads than the steep ones (columns 1 and 2). Comparing the rates for the flat levels of different shells we find a considerable increase with increasing  $n_x$  (columns 4 and 1). For geometry (ii) the states within one shell with equal quantum numbers  $n_x$  and  $n_y$  are most strongly coupled to the leads. However, the difference between strongly and weakly coupled states is not as pronounced as in geometry (i).

We conclude that *independently of the precise shape of the barrier*, in a geometry of type (i) which is realized in Figure 1 flat levels are more strongly coupled to the leads than steep levels. This is because the wave functions of flat levels have cigar-like shapes extending closer to the leads (cf. Figure 3). Therefore, flat levels carry the bulk of the current. The difference between well coupled and poorly coupled dot states is less pronounced when the leads are arranged at an angle (geometry (ii)). In this case, the mechanism for peak correlations described in Sec. II leads us to expect a reduction in the length of sequences of correlated peaks.

We present results for  $\alpha = 1$ ,  $\gamma = 0.005$ ,  $E_0 = -11$  and  $V_0 = 90$ . At zero deformation, the mean level spacing  $\Delta$  is related to the harmonic oscillator frequency  $\omega_x$  in  $x$ -direction by

$$\Delta = \frac{E_F}{N_{el}} = \frac{\hbar\omega_x N_{sh}}{\frac{1}{2}(N_{sh} + 1)(N_{sh} + 2)} \approx \frac{2\hbar\omega_x}{N_{sh}}. \quad (11)$$

Here  $N_{sh}$  is the number of the last filled shell and  $N_{el} = (N_{sh} + 1)(N_{sh} + 2)/2$  is the total number of electrons on the dot. We take  $N_{sh} = 14$  so that there are about 100 electrons on the dot. We assume  $\Delta = 0.03U$  which roughly corresponds to the situation of the experiments of Refs. [5,9].

In order to monitor the influence of a flat level  $F$  on the conductance, we define the distance  $d$  of  $F$  from the Fermi energy as the *number* of levels between  $F$  and the Fermi energy including  $F$  itself and count positively (negatively) for states above (below) the Fermi energy. Thus,  $d = 1$  indicates that  $F$  is the first unoccupied level. Figure 5 shows  $d$  vs. gate voltage for the flat level  $n_x = 14, n_y = 0$ . Adjacent points correspond to adjacent Coulomb

blockade resonances. For  $130 < V_g < 160$ ,  $F$  stays in the vicinity of the Fermi energy. Hence there is – on average – one crossing with a steep level in the interval  $\delta V_g$ . For  $V_g < 130$  ( $V_g > 160$ ), the number of avoided crossings in the interval  $\delta V_g$  is less than one (bigger than one), and  $F$  moves towards the (away from the) Fermi energy, respectively. The jumps at  $V_g = 156$  and  $V_g = 180$  are due to multiple crossings of levels which occur because of the integrability of our model.

For the same choice of parameters as in Figure 5 and for geometry (i), Figure 6 shows the conductance vs. gate voltage for two temperatures, (a)  $kT = 0.2\Delta$  and (b)  $kT = 0.4\Delta$ . About 100 Coulomb blockade resonances occur in the interval  $100 < V_g < 200$ . In both plots strong peaks with similar peak heights appear whenever the flat level  $F$  is close to the Fermi energy, especially at the higher temperature (case (b) of Figure 6). In the regions  $V_g < 130$  and  $V_g > 160$  where the conductance is not dominated by the flat level  $F$ ,  $G$  is much smaller than in the interval  $130 < V_g < 160$ . On the scale of Fig. 6, some of the conductance peaks are not even visible.

Figure 7 shows the conductance vs. gate voltage for the same parameters as in case (b) of Figure 6 but for geometry (ii). Now, the resonances are dominated by steeper levels from higher shells which are coupled more strongly to the leads than the flat level. This is why the peak heights are bigger on average than in Figure 6, why they show stronger variation, and why they increase systematically with increasing gate voltage.

#### IV. PHASE

We now turn to the behavior of the phase of the transmission amplitude through the quantum dot. This phase has recently been measured in a set of experiments using an Aharonov–Bohm (AB) interferometer with a quantum dot embedded in one of its arms. We consider the simplest case where the AB interferometer is coupled to only one channel in each connecting lead. The transmission coefficient  $\mathcal{T}$  through the AB device is then given by

$$\mathcal{T} \approx \mathcal{T}_0 + 2\text{Re} \left\{ t_0^* e^{-2\pi i \Phi / \Phi_0} \int dE \left( -\frac{\partial f}{\partial E} \right) t_{QD}(E) \right\}. \quad (12)$$

Here,  $\mathcal{T}_0 = |t_0|^2$  is a flux– and energy–independent term given by the square of the amplitude for transmission through the empty arm of the AB interferometer, while  $t_{QD}$  is the amplitude through the arm containing the dot. Since the quantum dot is weakly coupled to the arm, we have  $|t_{QD}| \ll |t_0|$ . We have explicitly displayed the dependence on the magnetic flux  $\Phi$  through the AB device and neglected higher harmonics. The symbol  $\Phi_0 = h/e$  denotes the elementary flux quantum.

The master equation used in Section III deals with occupation probabilities and is, therefore, not able to yield the phase of the transmission amplitude  $t_{QD}$ . We have used another approach. We have expressed  $t_{QD}$  in terms of the retarded Green function  $G^{\text{ret}}$  of the dot,

$$t_{QD}(E) = \sum_{i,j} V_i^L(E) G_{ij}^{\text{ret}}(E) V_j^{R*}(E). \quad (13)$$

The finite–temperature Green function  $G^{\text{ret}}$  must be calculated in the presence of the interaction  $U$  and the tunneling. A derivation of  $G^{\text{ret}}$  starting from the equations of motion is given in Appendix A. Assuming that the total number of electrons on the dot is a constant of motion, we obtain

$$G_{ij}^{\text{ret}}(E) \approx \delta_{ij} \sum_{N=0}^{\infty} P_N^{\text{eq}} \left[ \frac{1 - \langle \hat{n}_i \rangle_N}{E - (\epsilon_i - \mu + UN) + i\Gamma_i/2} + \frac{\langle \hat{n}_i \rangle_N}{E - (\epsilon_i - \mu + U(N-1)) + i\Gamma_i/2} \right]. \quad (14)$$

Here  $\Gamma_i = \Gamma_i^L + \Gamma_i^R$ . The probability  $P_N^{\text{eq}}$  that there are  $N$  electrons on the dot and the canonical occupation number  $\langle \hat{n} \rangle_N$  are given in Eqs. (8) and (9), respectively.

Within our approximations the Green function  $G^{\text{ret}}$  is diagonal. This fact implies that real ( particle–hole) excitations of the dot caused by tunneling transitions are not taken into account. This is justified in the regime of elastic cotunneling  $kT < \sqrt{U\Delta}$  where inelastic cotunneling processes do not contribute significantly to the transmission [2]. Equation (14) is a good approximation to the exact retarded Green function between Coulomb blockade resonances where fluctuations in the occupation number of the dot are strongly suppressed.

Moreover, *even at resonance* where  $G^{ret}$  reduces to a single Breit–Wigner term, Eq. (14) is expected [20] to apply provided there are no degeneracies and we work well above the Kondo temperature [21]. The success of Eq. (14) in these limiting cases suggests that well above the Kondo temperature, Eq. (14) is a good approximation to the exact Green function for all energies.

Combining Eqs. (14) and (12) we obtain

$$\mathcal{T} = \mathcal{T}_0 + \text{Re } t_0^* \widetilde{t_{QD}} e^{-2\pi i \Phi/\Phi_0}, \quad (15)$$

where

$$\begin{aligned} \widetilde{t_{QD}} &= \int dE \left( -\frac{\partial f}{\partial E} \right) t_{QD}(E) \\ &= \frac{\beta}{2\pi i} \sum_i \sum_{N=0}^{\infty} V_i^L V_i^{R*} P_N^{\text{ed}} \left[ (1 - \langle \hat{n}_i \rangle) \psi^{(2)} \left( \frac{\beta}{2\pi i} (i\Gamma_i - \epsilon_i + \mu - UN) + \frac{1}{2} \right) \right. \\ &\quad \left. + \langle \hat{n}_i \rangle \psi^{(2)} \left( \frac{\beta}{2\pi i} (i\Gamma_i - \epsilon_i + \mu - U(N-1)) + \frac{1}{2} \right) \right] \end{aligned} \quad (16)$$

with the trigamma function  $\psi^{(2)}$ .

In Figure 8 we show the phase  $\phi$  of the transmission amplitude versus gate voltage. As in the calculation of the conductance in Section III, the canonical occupation numbers are obtained by distributing 8 electrons over a window containing 16 levels. We take  $\Gamma_i = \Gamma = 0.002U = \Delta/15$ . The solid lines at the bottom of the plots show the conductance peaks and help to identify the resonance positions. In the left part of Figure 8 the flat level  $n_x = 14$ ,  $n_y = 0$  is close to the Fermi energy. Here we find a strikingly similar behavior of the phase at all resonances. This behavior is found not only within the  $V_g$  interval shown but *for the entire interval*  $130 < V_g < 160$  *comprising 30 resonances*. The phase regularly increases by  $\pi$  at resonance and displays a sharp lapse by  $\pi$  between adjacent resonances. As observed in Refs. [12,13] the increase at resonance occurs on the scale  $kT$  (we assume  $kT > \Gamma$ ) and the phase lapse between resonances on the scale  $\Gamma$ . The temperature dependence of the phase is shown in Figure 9. In the right part of Figure 8 we show the transmission phase for the case where the distance between the flat level and the Fermi energy is large compared to

$kT$  and increases with  $V_g$  (cf. Figure 5). The phase behaves less regularly, with an increase by  $\pi$  or less at and an immediate phase lapse near the resonances. Between resonances the phase remains virtually constant.

To interpret our results, we consider first the phase  $\phi$  at resonance. The identical behavior of  $\phi$  at all resonances in Figure 8(a) reflects the fact that at each resonance, the transmission through the dot is dominated by the strongly coupled level  $F$ . This is the same mechanism as in the sequence of strong conductance peaks shown in Figure 6(a). The more erratic phase behavior seen in Figure 8(b) is the result of the interplay of various levels of the dot. The regular behavior of the phase lapse between adjacent resonances is also due to the dominance of the flat level. At finite temperature the flat level  $F$  has a finite probability of being either occupied or empty and, thus, may contribute to both an electron-like and a hole-like cotunneling process. The contribution of both processes to the transmission amplitude through the dot is

$$t_F = V_F^L V_F^{R*} \left[ \frac{1 - \langle \hat{n}_F \rangle_N}{E - (\epsilon_F - \mu + UN) + i\Gamma_F/2} + \frac{\langle \hat{n}_F \rangle_N}{E - (\epsilon_F - \mu + U(N-1)) + i\Gamma_F/2} \right] \quad (17)$$

where the first (second) term represents the electron-like (hole-like) contribution, respectively. As the gate voltage  $V_g = \mu/\alpha$  scans the  $N^{\text{th}}$  valley (i.e. varies from  $(\epsilon_N + U \cdot (N-1))/\alpha$  to  $(\epsilon_{N+1} + U \cdot N)/\alpha$ ), the sign of  $\text{Re } t_F$  reverses, leading to a phase lapse. The same conclusion has previously been reached in Ref. [12]; an interpretation in terms of scattering theory has been given in Ref. [13]. If  $F$  is far away from the Fermi energy (on the scale of  $kT$ ) either the particle-like or the hole-like process will dominate, and the phase lapse moves from the valley towards the resonance, as depicted in Figure 8(b).

We emphasize that the phase lapse between resonances is a genuine interaction effect. Indeed, the interaction  $U$  is needed to keep the flat level close to the Fermi energy for a long sequence of resonances. For non-interacting particles ( $U \rightarrow 0$ ) the transmission amplitude at different resonances would be dominated by different single-particle levels. In the same limit, the cotunneling amplitude (17) would reduce to a single, temperature-independent term. The phases of the transmission amplitude in consecutive valleys would not be correlated,

and there would be no systematic phase lapse between resonances. We also note that the systematic phase lapse occurs only at finite temperature. At zero temperature a flat level could only contribute to either particle-like or hole-like cotunneling.

## V. SUMMARY. THE QUESTION OF NON-UNIVERSALITY

Since the first measurements on quantum dots in Aharonov-Bohm interference devices were reported, many aspects of phase-coherent transport through quantum dots have been understood theoretically. However, one of the most striking features, the strong correlations of the transmission phases in sequences of many resonances, has long withstood a satisfactory theoretical explanation. Earlier attempts [11,12] to solve the problem could account for short sequences but not for the sequences of more than 10 resonances found experimentally.

In this paper we have demonstrated the viability of a mechanism, based on a synthesis of the ideas proposed in Refs. [11,12], that gives rise to long sequences of correlated peak heights and transmission phases. We have used several approximations, the most central one being that the confining potential defining the dot is “almost” integrable. More precisely, both the deviation from integrability and the disorder must constitute a perturbation which is small on the scale of the mean single-particle level spacing. Our model shares many features of the ballistic quantum dots employed in some experiments [5,9] and may account semiquantitatively for some of the experimental observations. Nevertheless, our analysis naturally falls short of providing a complete and universal framework which could account for the combined effect of disorder and interaction on correlations in transmission experiments.

We have used the following specific conditions and assumptions: (i) Among the eigenstates of the quantum dot, some must be coupled more strongly to the leads than others. This assumption is met by a model which is nearly integrable, as is the case for our parabolic confining potential. This potential renders  $(n_x, n_y)$  good quantum numbers for all values of  $V_g$ . Of all levels in a shell, the level with  $n_y = 0$  is most strongly coupled to the leads. (ii) Changes in the gate voltage induce deformations of the dot boundary such that the po-

tential is deformed in the transverse  $y$ -direction. This assumption guarantees that in each shell, the level with  $n_y = 0$  is flat, i.e., stays close to the Fermi energy over a wide range of  $V_g$ -values. (iii) On average there is one crossing of the flat level with one other level per unit interval. This interval is defined by the change in  $V_g$  needed to add an extra electron to the dot. (iv) The temperature is sufficiently high to produce sufficiently long sequences of correlated resonances. The minimum temperature required by this condition depends both on the distance of the most strongly coupled level from the Fermi energy, and on the relative strength of the coupling of that level to the leads. With increasing temperature the correlations become more robust.

Strong boundary deformations leading to strongly chaotic classical motion within the dot, or strong disorder in the dot are likely to destroy the correlations altogether since they generically do not allow for the existence of eigenstates that are particularly well coupled to external leads. In this sense, the correlations proposed in the present paper are *non-universal in origin*. This conclusion agrees with the observation of weak peak correlations in the strongly deformed dots of Ref. [5] as compared with the strong correlations found in the experiments of Ref. [9].

Our ideas may be checked experimentally on dots that are not embedded in an AB device but are coupled directly to leads. This setup does not allow for tests of phase correlations but provides a convenient setup for measuring conductance peak correlations. The conductance of a dot with a regular (rectangular) lithographic shape has been measured by Simmel *et al.* [7]. These authors did indeed find a sequence of more than 10 strong peaks with very similar peak heights. In the same sweep they also observe envelopes of smaller peaks very similar to our results in Figure 6. To test our picture further, it would be illuminating to perform a similar two-terminal conductance experiment with leads attached at two sides of the dot which form an angle of 90 degrees. Here, a reduction of the correlations is to be expected. It would also be interesting to compare two setups, one with a plunger gate and the other with a backgate configuration. In the latter case the potential deformation is reduced. This should suppress our correlation mechanism.

## VI. ACKNOWLEDGMENT

This work was supported by the German-Israeli Foundation (GIF), by the Israel Science Foundation founded by the Israel Academy of Sciences and Humanities-Centers of Excellence Program, and by the U.S.-Israel Binational Science Foundation (BSF).

## APPENDIX A: RETARDED GREEN FUNCTION

We derive Eq. (14). The retarded Green function is defined as

$$G_{kl}^{ret} = -i\theta(t) \langle [c_k(t), c_l^\dagger(0)]_+ \rangle = F_{kl} + G_{kl} \quad \text{where} \quad (A1)$$

$$G_{kl} = -i\theta(t) \langle c_k(t) c_l^\dagger(0) \rangle \quad F_{kl} = -i\theta(t) \langle c_l^\dagger(0) c_k(t) \rangle. \quad (A2)$$

The brackets denote the thermal average,  $\langle \dots \rangle = \text{tr}(\dots \exp(-\beta H)) / \text{tr}(\exp(-\beta H))$ . With  $P_N = \text{tr}_N \exp(-\beta H) / \text{tr} \exp(-\beta H)$ , we write the trace as a sum of terms with a fixed number  $N$  of electrons on the dot,

$$G_{kl} = -i\theta(t) \sum_{N=0}^{\infty} P_N \langle c_k(t) c_l^\dagger(0) \rangle_N = \sum_{N=0}^{\infty} G_{kl}^{(N)}. \quad (A3)$$

In the “equation of motion” method the Green function is differentiated with respect to time. Since the time evolution of an operator is given by the commutator with the Hamiltonian, a system of differential equations containing higher-order Green functions is generated. A closed system is obtained if these Green functions can be approximately uncoupled. The solution is obtained by Fourier transformation. Specifically,

$$\frac{\partial}{\partial t} G_{ij}^{(N)} = -i\delta(t) \langle c_i(0) c_j^\dagger(0) \rangle_N - \theta(t) \langle [c_i, H](t) c_j^\dagger(0) \rangle_N \quad (A4)$$

$$= -i\delta(t) \langle c_i(0) c_j^\dagger(0) \rangle_N - \theta(t) \left( (\epsilon_i - \mu) \langle c_i(t) c_j^\dagger(0) \rangle_N + U \langle N(t) c_i(t) c_j^\dagger(0) \rangle_N \right) \\ - \theta(t) \sum_k \left( V_{ki}^{L*} \langle a_k(t)^L c_j^\dagger(0) \rangle_N + V_{ki}^{R*} \langle a_k(t)^R c_j^\dagger(0) \rangle_N \right). \quad (A5)$$

Since the interaction contains two creation and two annihilation operators a two particle Green function appears in the second line. The last two terms stem from the coupling to the leads, and by another equation of motion can be expressed in terms of the Green function

for the dot. Assuming that the states in the lead and in the dot are uncorrelated at  $t = 0$  we obtain

$$\langle a_k(t)c_j^\dagger(0) \rangle_N = \sum_i V_{ki}^L \int d\bar{t} G_{ij}^{(N)}(t - \bar{t}) \theta(\bar{t}) \exp(-i\epsilon_k^L \bar{t}) . \quad (\text{A6})$$

Fourier transformation of Eq. (A5) yields

$$\begin{aligned} \omega G_{ij}^{(N)} = & \langle 1 - n_i \rangle_N \delta_{ij} + (\epsilon_i - \mu) G_{ij}^{(N)} + U \tilde{G}_{ij} + \\ & + \sum_{kl} \left( \frac{V_{ki}^{L*} V_{kl}^L}{\omega - \epsilon_k^L + i\delta} + \frac{V_{ki}^{R*} V_{kl}^R}{\omega - \epsilon_k^R + i\delta} \right) G_{lj}^{(N)} \end{aligned} \quad (\text{A7})$$

where  $\tilde{G}_{ij} = -i \int dt \theta(t) \langle N(t) c_i(t) c_j^\dagger \rangle_N \exp i\omega t$ . The equations of motion are closed by assuming the total occupation  $N$  to be constant. Then the number operator can be taken out of the expectation value. The assumption is justified in the valleys between resonances whereas at each resonance,  $N$  fluctuates. For isolated resonances (level width  $\ll$  level spacing), we have  $\text{Im} \sum_k V_{ki}^{L*} V_{kl}^L / (\omega - \epsilon_k^L + i\delta) = -i\delta_{il} \Gamma_i^L / 2$ . This yields

$$G_{ij}^{(N)} = \frac{\delta_{ij} \langle 1 - n_i \rangle_N}{\omega - (\epsilon_i - \mu + UN) + i\Gamma_i^L/2 + i\Gamma_i^R/2} . \quad (\text{A8})$$

For  $F_{ij}$  we proceed analogously and eventually obtain Eq. (14).

## REFERENCES

- [1] For a review see: L.P. Kouwenhoven, C.M. Marcus, P.L. McEuen, S. Tarucha, R.M. Westervelt, and N.S. Wingreen in: Proceedings of the NATO Advanced Study Institute on Mesoscopic Electron Transport, edited by L.P. Kouwenhoven, L. Sohn and G. Schön (Kluwer Series E, 1997).
- [2] D.V. Averin and Yu.N. Nazarov, Phys. Rev. Lett. 76, 1695 (1990).
- [3] R. Jalabert, A.D. Stone and Y. Alhassid, Phys. Rev. Lett. 68, 3468 (1992).
- [4] A.M. Chang, H.U. Baranger, L.N. Pfeiffer, K.W. West and T.Y. Chang, Phys. Rev. Lett. 76, 1695 (1996).
- [5] J.A. Folk, S.R. Patel, S.F. Godijin, A.G. Huibers, S.M. Cronenwett and C.M. Marcus, Phys. Rev. Lett. 76, 1699 (1996).
- [6] U. Sivan, R. Berkovits, Y. Aloni, O. Prus, A. Auerbach and G. Ben-Yoseph, Phys. Rev. Lett. 77, 1123 (1996).
- [7] F. Simmel, T. Heinzel and D.A. Wharam, Europhys. Lett. 38, 123 (1997).
- [8] R. Berkovits and U. Sivan, Europhys. Lett. 41, 653 (1998).
- [9] R. Schuster, E. Buks, M. Heiblum, D. Mahalu, V. Umansky and H. Shtrikman, Nature 385, 417 (1997).
- [10] Y. Alhassid, M. Gokcedag and A.D. Stone, private communication.
- [11] G. Hackenbroich, W.D. Heiss and H.A. Weidenmüller, Phys. Rev. Lett. 79, 127 (1997).
- [12] Y. Oreg and Y. Gefen, Phys. Rev. B 55, 13726 (1997).
- [13] G. Hackenbroich and H.A. Weidenmüller, Europhys. Lett. 38, 129 (1997).
- [14] L. Brey, N.F. Johnson and B.I. Halperin, Phys. Rev. B 40, 10647 (1989); S.K. Yip, Phys. Rev. B 43, 1707 (1991); Q.P. Lie, K. Karrai, S.K. Yip, S. Das Sarma and H.D.

Drew, Phys. Rev. B 43, 5151 (1991); W.D. Heiss and R.G. Nazmitdinov, Phys. Rev. B. 55, 16310 (1997).

[15] C.B. Duke, *Tunneling in Solids* in Solid State Physics Suppl. 10, edited by F. Seitz, D. Turnbull and H. Ehrenreich. Academic Press 1969.

[16] P.W. Anderson, Phys. Rev. 124, 41 (1961).

[17] G. Hackenbroich and H.A. Weidenmüller, Phys. Rev. B 53, 16379 (1996).

[18] C.W.J. Beenakker, Phys. Rev. B 44, 1646 (1991).

[19] Y. Meir, N.S. Wingreen and P.A. Lee, Phys. Rev. Lett. 66, 3048 (1991).

[20] C.A. Stafford, Phys. Rev. Lett. 77, 2770 (1996).

[21] L.I. Glazman and M.E. Raikh, Pis'ma Zh. Eksp. Teor. Fiz. 47, 378 (1988) [JETP Lett. 47, 452 (1988)]; H. Schoeller and G. Schön, Phys. Rev. B 50, 18436 (1994); A. Kamenev and Y. Gefen, Phys. Rev. B 54, 5428 (1996).

TABLES

$n = (n_x, n_y)$	(14,0)	(0,14)	(6,8)	(12,0)	(6,6)
$\Gamma_n$ for geometry (i)	$2.68 \cdot 10^{-6}$	$4.04 \cdot 10^{-23}$	$5.34 \cdot 10^{-14}$	$9.09 \cdot 10^{-8}$	$6.11 \cdot 10^{-14}$
$\Gamma_n$ for geometry (ii)	$6.30 \cdot 10^{-12}$	$6.30 \cdot 10^{-12}$	$5.66 \cdot 10^{-7}$	$2.88 \cdot 10^{-12}$	$2.41 \cdot 10^{-8}$

TABLE I. Tunneling rates for several levels  $n$  calculated from Eq. (10). In geometry (i) the leads are opposite to each other with  $\xi_x = \sqrt{50}$  and  $\xi_y = 0$ . In geometry (ii), the leads are arranged at an angle, with  $\xi_x = \xi_y = \sqrt{50/2}$ .

## FIGURES

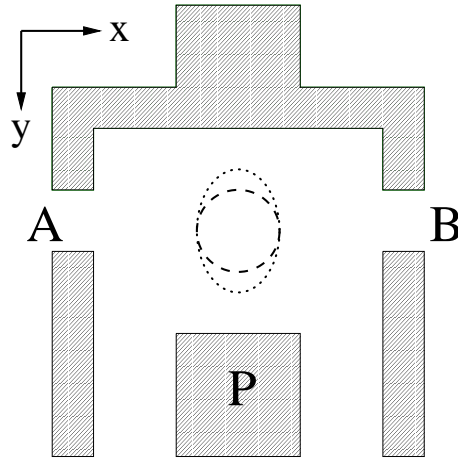


FIG. 1. A quantum dot (schematic). Electrons enter or leave the dot through the tunneling barriers  $A$  and  $B$ . The plunger gate  $P$  controls the number of electrons on the dot. Equipotential lines of the confining potential are shown for the isotropic (dashed) and deformed (dotted) case.

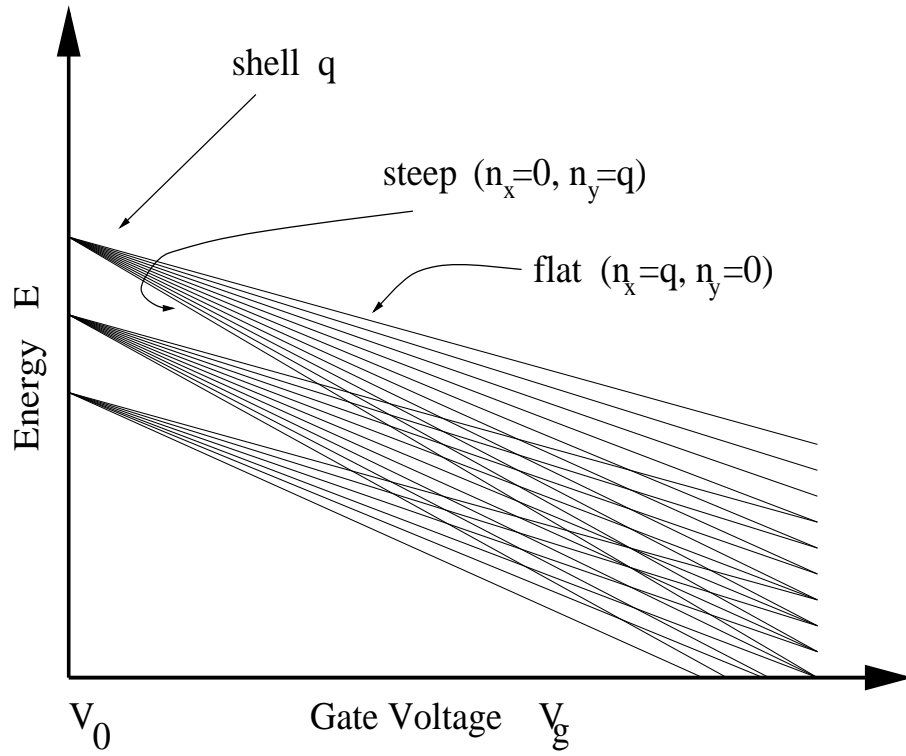


FIG. 2. Dependence of the single-particle energies of the dot on the gate voltage  $V_g$ .

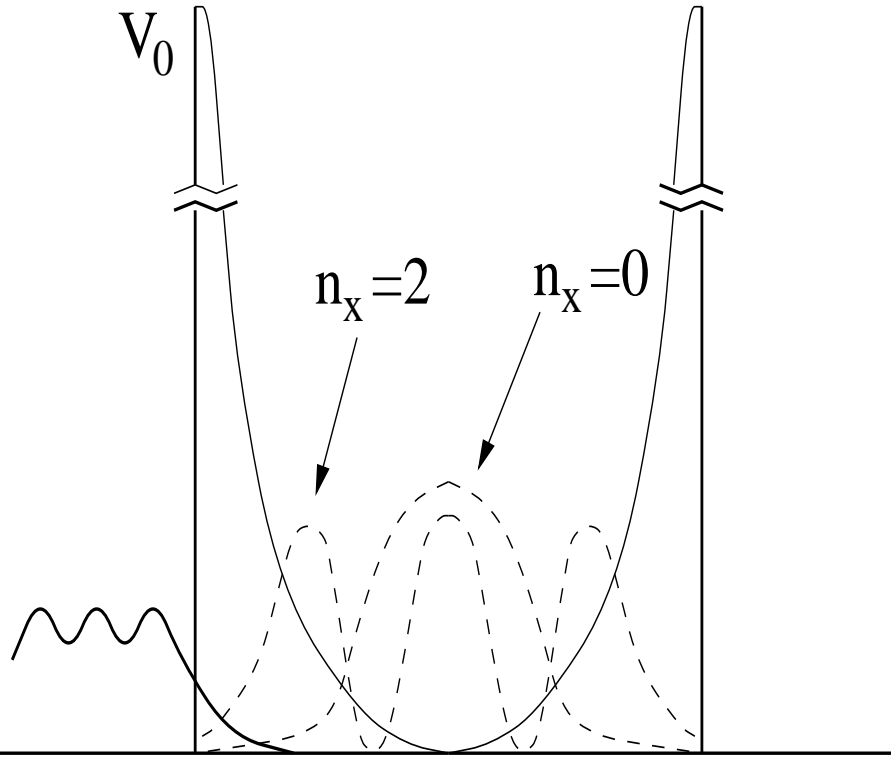


FIG. 3. The thin solid line shows a cross section of the potential in longitudinal direction, the two barriers lying at opposite ends. The overlap of the dot wave functions (probability shown as dashed lines) and of the lead wave function (probability shown as a solid line on the left) increases strongly with the quantum number  $n_x$  in x-direction.

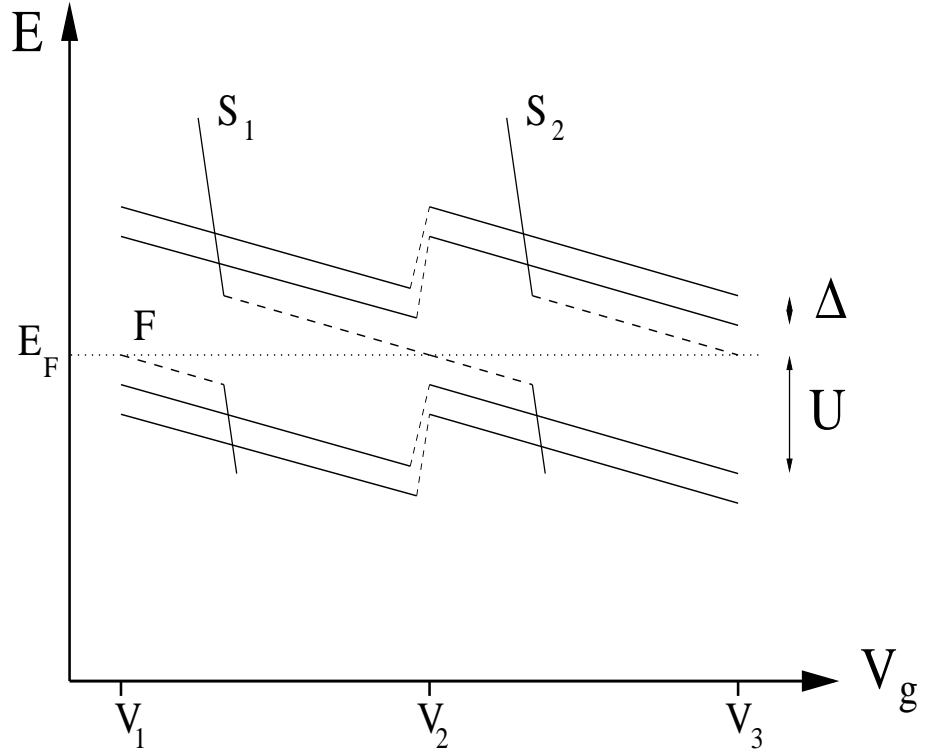


FIG. 4. Avoided crossings with the steep levels  $S_1$  and  $S_2$  cause the flat level  $F$  (dashed) to stay close to the Fermi energy  $E_F$ . Resonances dominated by this level occur at gate voltages  $V_1, V_2, V_3$ . There is a gap of magnitude  $U$  between the last occupied and the first empty level.

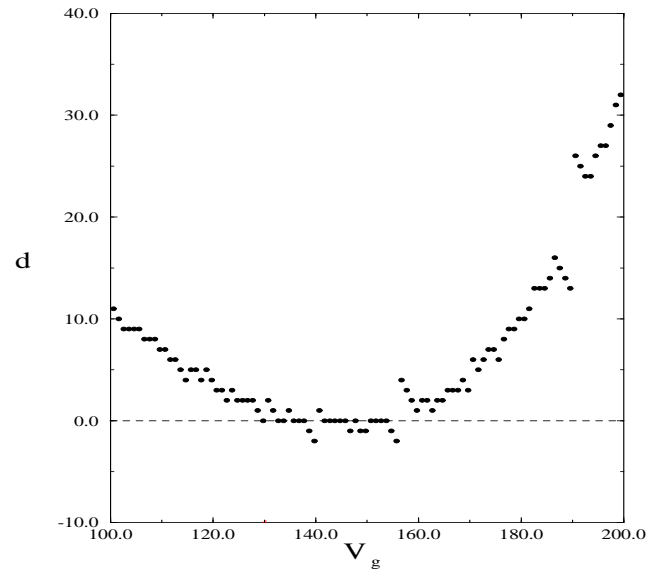


FIG. 5. Distance  $d$  (in number of levels) of the flat level ( $n_x = 14, n_y = 0$ ) from the Fermi energy  $E_F$  versus gate voltage  $V_g$ .

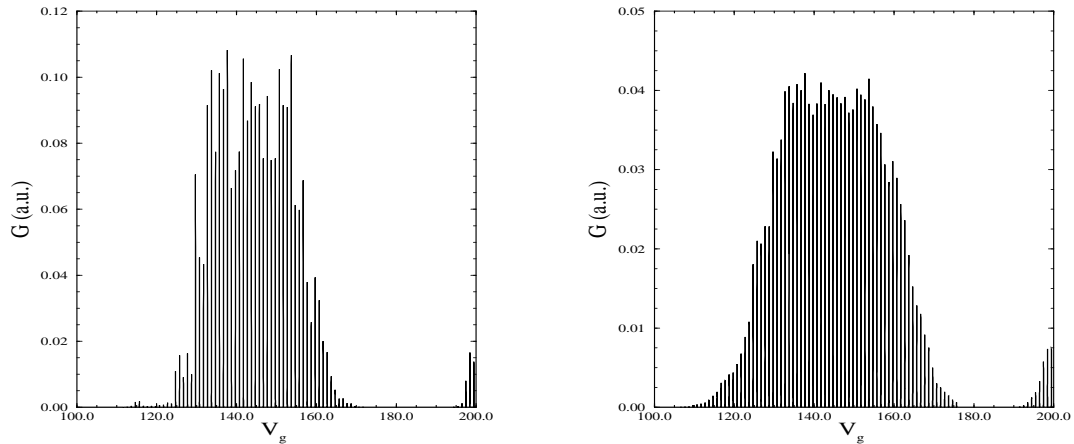


FIG. 6. Conductance  $G$  vs. gate voltage for (a)  $kT = \Delta/5$  (left) and (b)  $kT = 2\Delta/5$  (right).

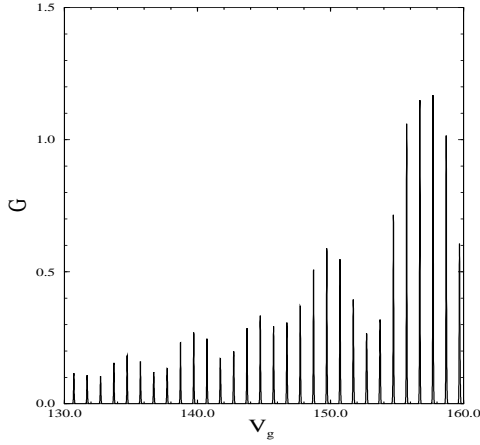


FIG. 7. Conductance  $G$  vs. gate voltage  $V_g$  for the same parameters as in Figure 6 (b) but with the leads arranged at an angle of 90 degrees.

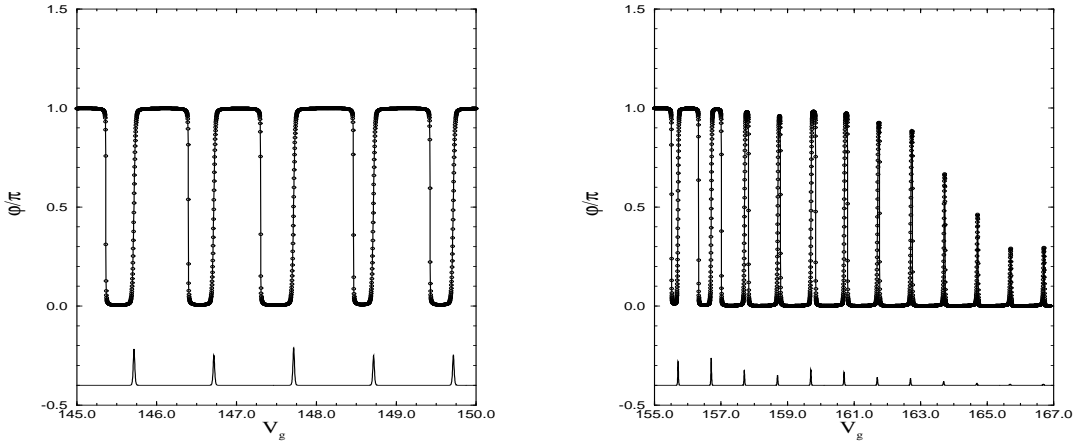


FIG. 8. Phase  $\phi$  of the transmission amplitude versus gate voltage  $V_g$  at  $kT = \Delta/5$  in two different intervals. The solid lines at the bottom of the plots display the conductance peaks. In the case shown in the left (right) part, the flat level  $n_x = 14, n_y = 0$  is at or near (far removed from) the Fermi level, respectively. In the case of the right part, the flat level influences the phase as a background only.

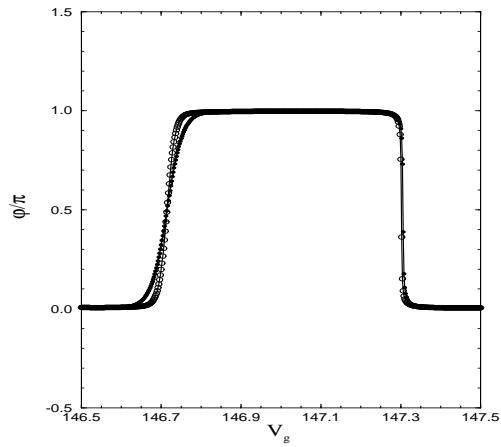


FIG. 9. Transmission phase for  $kT = 0.2\Delta$  (open circles) and  $kT = 0.4\Delta$  (filled circle). The increase by  $\pi$  at the resonance takes place on the scale  $kT$ , the phase lapse between resonances, on the scale  $\Gamma$ .